How to cite: *Angew. Chem. Int. Ed.* **2024**, *63*, e202405246
doi.org/10.1002/anie.202405246

VIP Photoswitching Very Important Paper

Photoswitching Reagent for Super-Resolution Fluorescence Microscopy

*Ga-eun Go, Uidon Jeong, Hyunbum Park, Seokran Go, and Doory Kim**

Abstract: Single-molecule localization microscopy (SMLM) has revolutionized optical microscopy by exceeding the diffraction limit and revealing previously unattainable nanoscale details of cellular structures and molecular dynamics. This super-resolution imaging capability relies on fluorophore photoswitching, which is crucial for optimizing the imaging conditions and accurately determining the fluorophore positions. To understand the general on and off photoswitching mechanisms of single dye molecules, various photoswitching reagents were evaluated. Systematic measurement of the single-molecule-level fluorescence on and off rates (k_{on} and k_{off}) in the presence of various photoswitching reagents and theoretical calculation of the structure of the photoswitching reagent-fluorophore pair indicated that the switch-off mechanism is mainly determined by the nucleophilicity of the photoswitching reagent, and the switch-on mechanism is a two-photon-induced dissociation process, which is related to the power of the illuminating laser and bond dissociation energy of this pair. This study contributes to a broader understanding of the molecular photoswitching mechanism in SMLM imaging and provides a basis for designing improved photoswitching reagents with potential applications extending to materials science and chemistry.

[*] G.-e. Go, U. Jeong, H. Park, S. Go, D. Kim
Department of Chemistry
Hanyang University
Seoul 04763, Republic of Korea
E-mail: doorykim@hanyang.ac.kr

D. Kim
Research Institute for Convergence of Basic Science
Institute of Nano Science and Technology, and Research Institute for Natural Sciences
Seoul 04763, Republic of Korea

Introduction

Single-molecule localization microscopy (SMLM), a representative category of super-resolution microscopy, has revolutionized optical microscopy by overcoming the diffraction limit, which is a fundamental barrier to traditional light microscopy.[1–6] The development of SMLM has advanced the contemporary understanding of biology, enabling researchers to study the organization of molecules and complexes within cells on the nanoscale in unprecedented detail.[7–9] Recently, SMLM has opened up new applications across various scientific disciplines. Such applications include semiconductor and polymer nanostructures, enabling research into the nanoscale properties of nanomaterials.[10–14] The super-resolution imaging capability of SMLM is based on fluorophore photoswitching, which enables precise localization of the individual fluorophore molecules and the reconstruction of super-resolved images.[15] Therefore, understanding the photoswitching of fluorophores is important because this phenomenon is a fundamental aspect of SMLM techniques such as stochastic optical reconstruction microscopy (STORM) and photoactivated localization microscopy (PALM).[4,5] Understanding the photoswitching mechanism enables researchers to optimize the imaging conditions, such as the laser parameters, imaging protocols, and detection schemes, to take full advantage of the photoswitching phenomenon, ultimately resulting in improved spatial resolution.[16,17] Understanding the photoswitching mechanism is also essential for accurately determining and quantifying the positions and intensities of individual fluorophores.[18] This quantification is crucial in biological research, as it enables precise analysis of cellular structures, protein distributions, and their dynamics. Understanding the photoswitching properties of fluorophores will also aid in developing better fluorophores for SMLM with specific photoswitching properties, such as brighter on-states and more reliable off-switching, thereby enhancing imaging capability.[19] This knowledge can lead to a deeper understanding of molecular photophysics and broader applications in fields such as materials science and chemistry.

Given the significance of understanding the photoswitching properties of fluorophores, many groups have proposed various molecular photoswitching mechanisms for fluorescent dyes.[20,21] To reconcile the seemingly divergent results reported by several groups, efforts have recently been made to unify the different mechanisms for thiol-induced photoswitching of cyanine dyes, which are the most utilized dyes for SMLM. However, these studies focused only on thiol-

induced photoswitching, particularly during the switching-off step.[20–24] For example, a reversible transition occurs between the fluorescent and dark transient states, in which the formation of a nonemissive cyanine dye-thiolate (Cy–SR) adduct is mainly responsible for the switching-off step. However, the detailed mechanism by which the fluorescent state is recovered remains unclear. Previous studies only considered thiols as photoswitching reagents; therefore, photoswitching reagents for SMLM have thus far been limited to thiols.

Herein, by focusing on the recovery switch-on step of the Alexa Fluor 647 dye, which is one of the most commonly used fluorescent dyes for STORM,[25] we propose a unified mechanism for photoswitching by analyzing various photoswitching reagents. To generalize the photoswitching mechanism of the dye induced by other molecules, various photoswitching reagent candidates, such as thiols (2-mercaptoethylamine (MEA), dithiothreitol (DTT)), amines (alanine, glycine), ethanol, hydrogen peroxide, halogenated benzene compounds (chlorobenzene, iodobenzene), and hydride compound (sodium hydride) are evaluated. The data show that the two-photon effect detaches the photoswitching reagent from the dye molecule during recovery to the fluorescent state, which explains why high laser power is required for fast photoswitching in STORM imaging. Theoretical calculations suggest that this multiphoton excitation is followed by dissociation in the excited state, allowing spontaneous recovery of the dye from the dark-state dye-photoswitching reagent adduct. Owing to this multiphoton-induced dissociation of the adduct in the off-to-on recovery process, dye molecules that are more strongly attached to the photoswitching reagent molecule tend to remain in the dark state longer and undergo fewer photoswitching cycles. Moreover, in the presence of bulky photoswitching reagent molecules, the dye molecules tend to remain in the fluorescent on-state longer because the bulky photoswitching reagent molecule has limited access to the dye molecule. Based on this systematic investigation of various photoswitching reagents, we tested NaN_3 as a new photoswitching reagent and successfully demonstrated super-resolution imaging of microtubules, mitochondria, and clathrin-coated pits (CCPs) with it. This systematic study of the dye photoswitching properties in the presence of various photoswitching reagent candidates is expected to enable the optimal design of new photoswitching agents and improve super-resolution imaging.

Results and Discussion

Mechanism of Dye Recovery to Fluorescent State via Two-Photon-Induced Dissociation of Photoswitching Reagent from Dye Molecule

First, we focused on the mechanism of recovery to the fluorescent state of the dye, which remains relatively unclear. Although it has been known that dye recovery could occur by either photoinduced or thermal elimination of the thiol from the dye-thiol adduct, the detailed mechanism has not been investigated. The questions of what determines and accelerates this recovery process and how laser illumination can induce the dissociation of thiol from the dye-thiol adduct remain unanswered (Figure 1a).

Before investigating this mechanism, we first examined the formation of the dye-photoswitching reagent adduct using UV/Vis absorption spectroscopy and mass spectrometry. As shown in Figure S1, we observed a decreased absorption peak intensity of Alexa Fluor 647 (AF647) (647 nm) and a newly formed blue-shifted peak intensity (200–400 nm) with the addition of the photoswitching reagent from both the simulated and experimental UV/Vis absorption spectra, implying the formation of a dark state by the AF647-photoswitching reagent adduct. We could also observe the formation of the AF647-photoswitching reagent adduct from mass spectra by accelerating its addition at high pH (Figure S1). Based on this evidence, we next investigated the mechanism of the off-to-on recovery step. We initially measured k_{on} with a variation of the excitation laser power (0.15–1.7 kW/cm^2). The rate of the recovery switch-on process has been considered first-order in previous studies.[20,22] As shown in Figure 1b, the recovery rate (k_{on}) increases as the excitation laser power increases. Notably, at a significantly low laser power (0.15 kW/cm^2), the dark state of the dye (possibly the dye-thiol adduct) tended to persist for longer, resulting in a very slow recovery rate (k_{on}). By contrast, at a high laser power (>0.85 kW/cm^2), the dark state of the dye could be quickly converted to the fluorescent state, resulting in the fast photoswitching required for super-resolution imaging. This not only explains why a high laser power is required for SMLM imaging but also suggests that the probability of dissociation of the thiol from the dye-thiol adduct is related to the photon energy. Interestingly, the slope of the log-scale graph of k_{on} versus the laser power was approximately 2, suggesting a two-photon process for the off-to-on recovery process. This two-photon dye-fluorescence recovery process is consistent with the high laser power required to activate the dye from the dark state.[26] The effect of additive UV illumination in this process was also evaluated by excitation using a 405 nm laser with a power of 17–51 W/cm^2 combined with low-power (0.15–0.2 kW/cm^2) laser excitation (647 nm). As shown in Figure 1b, even UV illumination with a low laser power (0.15–0.2 kW/cm^2) could accelerate this process by increasing k_{on}. Therefore, accelerated photoswitching of the dye was achieved using UV illumination at a low laser power (~0.2 kW/cm^2) combined with excitation using a low-power (0.15–0.2 kW/cm^2) laser (647 nm). The recovery of the dye to the fluorescent state by UV irradiation is also consistent with the previously observed photoactivation of the reduced dyes by UV light.[16] Therefore, the recovery of the dye from the dark state to the fluorescent state via dissociation of the thiol from the dye-thiol adduct can prospectively be induced by blue photons (in the UV range) even under excitation with a low-power laser or two photons of a red laser, which can explain why high laser power excitation or UV activation is required to activate the switching-on phenomena of dyes.

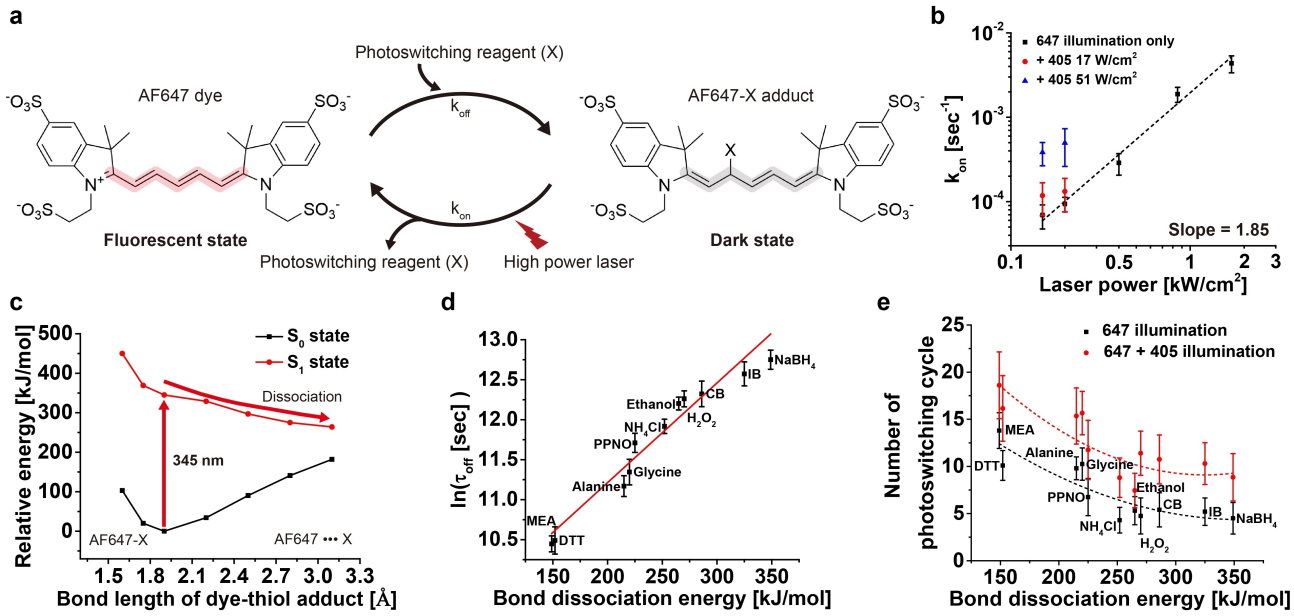

Figure 1. Proposed two-photon-induced off-to-on photoswitching mechanism in single-molecule localization imaging. (a) Photoswitching mechanism and associated rates and lifetimes. (b) Dependence of k_{on} on excitation laser (647 nm) power. Red and blue: k_{on} measured under simultaneous illumination with 647 nm excitation laser at a power of 0.15–1.7 kW/cm^2 and 405 nm activation laser at a power of 17–51 W/cm^2. ($n=5$, mean±SD) (c) Profiles of the relaxed potential energy surface (PES) of AF647-thiol adduct along the bond length coordinates showing the dissociative curve for the first excited state. PES for the ground state was calculated by DFT at the B3LYP/6-31+G(d,p) level and those for the excited states by TD-DFT at the same level. (d) Measured τ_{off} depending on the calculated dissociation energy for the bond between dye and photoswitching agent. ($n=40$, mean±SD) MEA: 2-mercaptoethylamine, DTT: dithiothreitol, PPNO: 4-phenylpyridine *N*-oxide, CB: chlorobenzene, IB: iodobenzene. (e) Number of photoswitching cycles of photoswitching reagents depending on the calculated dissociation energy for the bond between dye and photoswitching agent. ($n=40$, mean±SD)

To further investigate the mechanism of dissociation of the bond between the dye molecules and thiols induced by laser illumination, the ground and first excited states of the dye-thiol adduct were determined from theoretical calculations. Interestingly, a dissociative energy curve was constructed for the first excited state (Figure 1c). Therefore, the simulated potential energy diagram shows that once the dye-thiol adduct is excited to the first excited state, it quickly follows the dissociation curve, resulting in the dye and thiol molecules dissociation. The energy required for excitation from the ground state (S_0) to the first excited state (S_1) was calculated as ~345 nm, which is higher than the energy of the red light (647 nm) and approximately two-photon energy of the 647 nm light. As the length of the bond (C–S bond) between the dye molecule and thiol increases, the excitation energy decreases, as shown in Figure 1c. Thus, 405 nm photons are also expected to excite the dye-thiol molecules to the dissociated excited state. When the thiol is attached to the dye molecule in neutral form (R–SH), which is different from the deprotonated form (R–S$^-$), the calculated excitation energy is even lower (~560 nm) (Figure S2). In this case, a blue photon (405 nm), even with low power, could induce dissociation of the dye–thiol pair.

To confirm the proposed two-photon mechanism of bond dissociation in the dye-photoswitching reagent leading to the recovery of the dye to the fluorescent state, various photoswitching reagent candidates that interact with the dye molecule with different binding energies were evaluated (Figure S3a). As discussed above, prior studies on the photoswitching mechanism considered only thiol as a photoswitching agent, limiting further development of new photoswitching reagents. To generalize the photoswitching mechanism, various molecules that could interact with the dye molecule with different binding energies were selected as photoswitching reagent candidates, including thiol (MEA, DTT), amine (alanine, glycine), hydroxyl (ethanol, hydrogen peroxide), halogenated benzene (chlorobenzene, iodobenzene), and hydride (sodium hydride) groups. To assess the effect of the bond energy between the photoswitching reagent and dye molecule on recovery of the dye to the fluorescent state, the lifetime (τ_{off}) of the dark state (i.e., dye-photoswitching reagent adduct) was measured at the single-molecule level. The measured τ_{off} was plotted as a function of the calculated energy of the bond between the reagent and dye molecule, as shown in Figure 1d. Interestingly, photoswitching reagents with strong bond energies, such as BH_4^-, exhibited long dark-state lifetimes, whereas those with weak bond energies, such as thiols (MEA, DTT), exhibited short dark-state lifetimes. Therefore, photoswitching reagent candidates interacting with the dye molecule with high binding energies tend to remain in the off-state longer, making recovery to the fluorescent state difficult. This suggests that the energy for dissociation of the bond between the dye and photoswitching reagent molecule determines the lifetime of the dark state in the dye recovery process, which is consistent with the proposed mechanism.

Based on the assumption that the activation energy for dye recovery is approximately equal to the energy for dissociation of the bond between the dye and photoswitching reagent, a linear relationship between the bond dissociation and ln(τ_{off}) is expected (Figure S3b). We observed that the plot of ln(τ_{off}) versus the bond dissociation energy was linear (Figure 1d), again confirming that the bond dissociation process is the main factor influencing the fluorescence recovery.

Given the significant role of the binding energy between the dye and photoswitching reagent molecule in the fluorescence recovery process (i.e., the off-to-on process), we proposed that the binding energy could affect the number of photoswitching cycles. To investigate this effect, the number of switching cycles was measured for various photoswitching reagent candidates that bind to the dye molecules with different energies (Figure 1e). As the binding energy between the dye and photoswitching reagent increases, it becomes more challenging to induce a reversal from the dark state to the fluorescent state by laser illumination, reducing the number of photoswitching cycles. For example, in the presence of BH_4^-, the dye undergoes a few photoswitching cycles (average of ~2.5), plausibly due to the strong bonding between H^- and the dye molecule. Such strong bonding between H^- and the dye molecule can also be observed even when the hydride ion is added to the indolenine carbon, not to the polymethine bridge, which has been observed in previous study.[27] Although the second carbon on the polymethine bridge has been known to be the most plausible position for addition of reducing molecule,[16,20,21] a hydride ion is expected to be added to the sterically hindered indolenine carbons because of their small sizes. We also observed the predominant formation of hydrocyanine by the addition of a hydride ion to the indolenine carbon rather than the formation of hydrocyanine by the addition of a hydride ion to the second carbon on the polymethine bridge based on its relatively red-shifted absorption peak compared to other dye-photoswitching reagent adducts in the simulated and experimental UV/Vis absorption spectra (Figure S1). The bond dissociation energy of the hydrocyanine formed by the addition of hydride ion to the indolenine carbon was calculated as 425 kJ/mol, which is the strongest bond dissociation energy among all of the tested photoswitching reagents, still explaining the longest τ_{off} and smallest number of photoswitching cycles in our observation. Interestingly, this small number of photoswitching cycles could be increased by additional activation with UV light (405 nm), implying enhanced reversibility under high-energy laser illumination.

Overall, the results indicate that the fluorescent off-to-on process and the reversibility of photoswitching are mainly determined by the energy of the bond between the dye and photoswitching reagent molecules.

Switching-Off Mechanism Determined by Nucleophilicity of Photoswitching Reagent

The changes in the on-to-off kinetics of the dye were systematically investigated for various photoswitching reagents that have not been previously assessed. Based on a previously suggested mechanism for thiol addition to the dye molecule,[20] we proposed that the steric hindrance of the photoswitching reagent could affect the on-to-off photoswitching process because it is the main factor determining nucleophilicity. Therefore, the effect of steric hindrance of the photoswitching reagent (in the dye-reagent adduct) on the lifetime (τ_{on}) of the fluorescence on-state was evaluated (Figure 2).

As a well-known metric of the steric hindrance, the cone angle was determined from theoretical calculations.[28] As expected, in the presence of a photoswitching reagent with a high cone angle, the dye tended to remain in the fluorescent state longer, resulting in a longer "τ_{on}" because the bulky photoswitching reagent may not be effectively attached to the conjugated bond in the dye molecule. For example, photoswitching reagents with bulky functional groups, such as chlorobenzene, 4-phenylpyridine *N*-oxide, and iodoben-

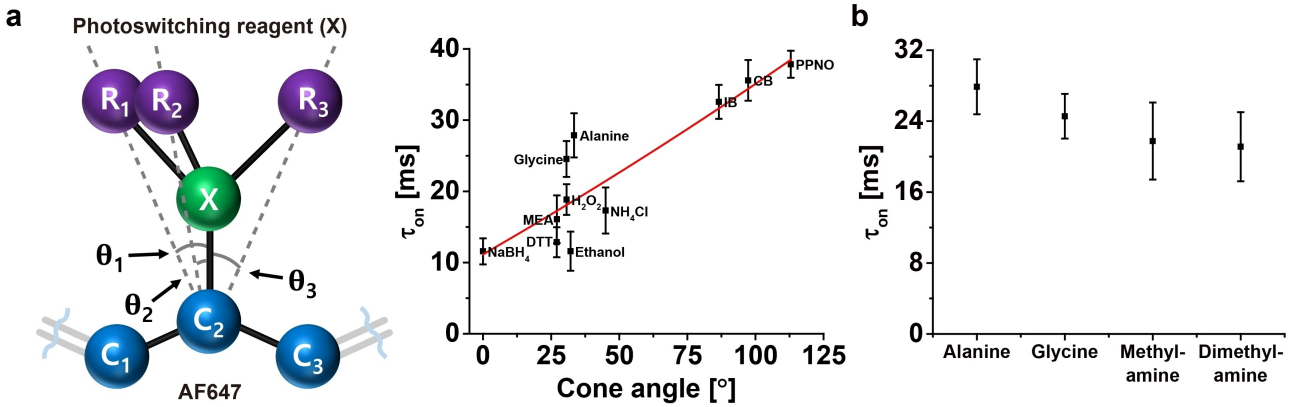

Figure 2. Effect of the nucleophilicity of photoswitching agent on the on-to-off photoswitching mechanism in single-molecule localization imaging. (a) Effect of steric hindrance (in terms of cone angle) on τ_{on}. The measurement of the cone angle is also shown on the left. ($n=40$, mean±SD) MEA: 2-mercaptoethylamine, DTT: dithiothreitol, PPNO: 4-phenylpyridine *N*-oxide, CB: chlorobenzene, IB: iodobenzene. (b) Measured lifetime of fluorescence-on state (τ_{on}) in the presence of various amine molecules with different substituents. ($n=40$, mean±SD)

zene, tend to remain in the fluorescent-on state longer because of poor interaction with the dye molecules. By contrast, the photoswitching reagents with a low cone angle, such as BH_4^-, exhibit a shorter "τ_{on}" as the addition of such a light photoswitching reagent to the dye molecule is facile. Therefore, the bulkiness of the photoswitching reagent is one of the main factors determining the on/off photoswitching mechanism through control of the accessibility to the dye molecule.

In addition to the steric hindrance effect, substituents on the nucleophile can affect the nucleophilicity. For example, molecules with benzene groups, such as 4-phenylpyridine *N*-oxide, chlorobenzene, and iodobenzene, are less nucleophilic because of delocalization of the nucleophilic lone pair by resonance. The effect of the nucleophilicity on the dye could be observed in the presence of these benzene molecules, where the lifetime (τ_{on}) of the fluorescence on-state was longer, suggesting low nucleophilicity. Because a longer fluorescence-on lifetime could result in a high probability of point spread function (PSF) overlapping with long lifetimes, a photoswitching reagent with a nucleophilic lone pair electron in the resonance group would not be preferable for single-molecule imaging. In addition, the nucleophilicity of the amine group is known to decrease in the presence of electron-withdrawing groups, such as carboxylic groups. Such an effect was also observed from the measurement of the fluorescence-on lifetime (τ_{on}) for photoswitching reagents with amine groups. In the presence of photoswitching reagents with carboxylic groups, such as alanine and glycine, the fluorescence-on lifetime (τ_{on}) of the dye increases, compared to the lifetime in the presence of other photoswitching reagents having a similar cone angle, as shown in Figure 2a. To confirm this, the fluorescence-on lifetime (τ_{on}) of the dye in the presence of methylamine or dimethylamine, having one or two electron-donating methyl groups was also measured. In the presence of these reagents (Figure 2b), the lifetime (τ_{on}) of the fluorescence-on state was shorter, suggesting the high nucleophilicity of these reagents compared to that of the amine molecules with electron-withdrawing groups, such as glycine and alanine. This suggests that the nucleophilicity of the photoswitching reagent plays a significant role in determining the fluorescence on-to-off process. Meanwhile, no clear relation between pK_a and τ_{on} was observed, suggesting that the basicity of the photoswitching reagent does not directly affect the fluorescence-on lifetime. (Figure S4). Collectively, the data indicate that the nucleophilicity of the photoswitching reagent, rather than the basicity, is the main factor determining the fluorescence-on lifetime (τ_{on}) during the photoswitching process.

STORM Image Quality of Biological Samples Depending on Type of Photoswitching Agent

We investigated the STORM image quality of biological samples based on systematic quantification of the photoswitching process for various photoswitching agents. The tested photoswitching reagents were roughly divided into four categories depending on their binding energy to the dye molecule and nucleophilicity: (Type 1) photoswitching reagents with weak binding energy and good nucleophilicity (i.e., MEA and DTT). (Type 2) Photoswitching reagents with intermediate binding energy and poor nucleophilicity (i.e., glycine and alanine). (Type 3) Photoswitching reagents with strong binding energy and good nucleophilicity (i.e., BH_4^-). (Type 4) Photoswitching reagents with strong binding energy and poor nucleophilicity (i.e., chlorobenzene and iodobenzene). The photoswitching properties of each type of photoswitching reagent are summarized in Table S1, facilitating the comparison of various photoswitching reagents. Given the measured photoswitching rates, photon numbers, and localization precision for each type of photoswitching reagent, it is expected that Type 1 would induce the best photoswitching properties in the AF647 dye, whereas Type 4 would exhibit the poorest photoswitching properties. To assess the STORM image quality, we performed STORM imaging of AF647-labeled microtubules in the presence of each type of photoswitching agent and measured the width and one-dimensional localization density of the microtubule filaments from the STORM images (Figure 3).

As expected, Type 1 photoswitching reagent, having weak binding energy and good nucleophilicity, generated the best STORM image quality by showing the hollow structure of the microtubules with narrow width and high localization density. The high-resolution STORM image of the hollow and narrow microtubule filaments results from the fast photoswitching process (high k_{on} and k_{off}), which is consistent with the single-molecule measurements. In addition, the high localization density resulting from the high number of photoswitching cycles contributes to the high resolution of the STORM images when Type 1 photoswitching reagents are used, consistent with the previously described our single-molecule measurement. The observation of such hollow microtubule filaments was compromised when Type 2 photoswitching reagents, which have intermediate binding energy and poor nucleophilicity, were used. Because both photoswitching-on and photoswitching-off processes of the dye in the presence of Type 2 reagents are relatively slower than those in the presence of Type 1 reagents, the localization density of the microtubules in the STORM images taken with the Type 2 photoswitching agent was lower than that of the image acquired with the Type 1 reagent. Type 2 reagents often show overlapping PSFs during STORM imaging, probably because of slower k_{on} and k_{off}, resulting in thick microtubule filaments. Such overlapped PSFs were rarely observed in the presence of the Type 3 reagent, which has a strong binding energy and good nucleophilicity, owing to the short lifetime of the fluorescence-on state (τ_{on}). However, the low number of photoswitching cycles resulting from the strong binding energy to the dye results in a low localization density of the microtubule filaments, which limits the quality of the STORM images. Finally, Type 4 photoswitching reagents with strong binding energy and poor nucleophilicity generated the worst STORM image quality because they contributed to the slowest k_{on} and k_{off} among the reagent types. Because of the long lifetime of the fluorescence-on state,

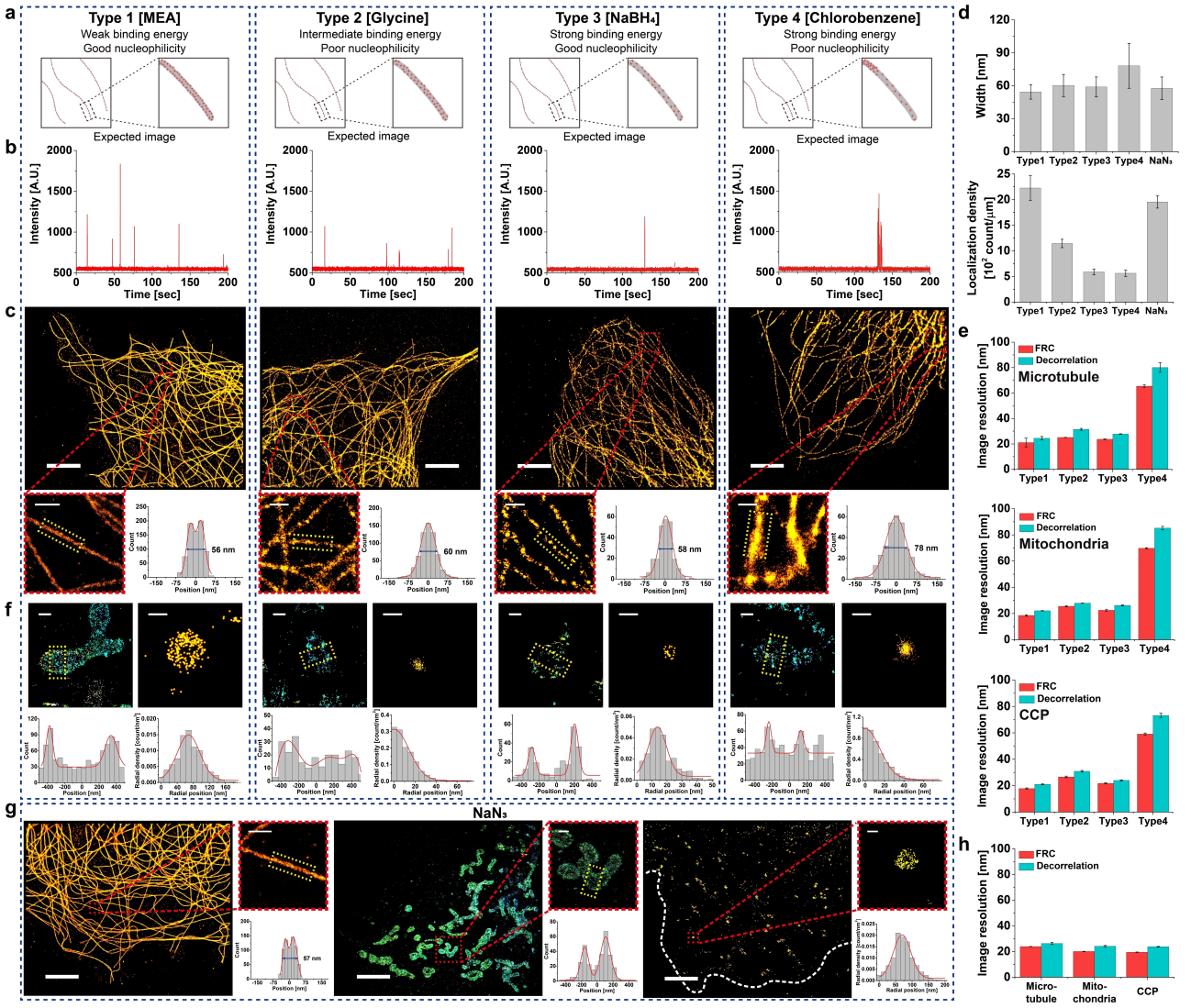

Figure 3. Effect of the binding strength to dye molecule and nucleophilicity of photoswitching agent on STORM image quality. (Type 1) Photoswitching agent with weak binding energy and good nucleophilicity (MEA, DTT). (Type 2) Photoswitching agent with intermediate binding energy and mild nucleophilicity (glycine, alanine). (Type 3) Photoswitching agent with strong binding energy and good nucleophilicity (BH_4^-). (Type 4) Photoswitching agent with a strong binding energy and poor nucleophilicity (chlorobenzene, iodobenzene). (a) Expected STORM image quality of an example structure using different types of photoswitching reagents (hollow tubule objects such as dye-labeled microtubules). (b) Representative single-molecule fluorescence-time traces for Alexa Fluor 647 in the presence of different types of photoswitching reagents. (c) Representative STORM images of microtubules labeled with Alexa Fluor 647 in the presence of different types of photoswitching reagents. Magnified images of red, dashed boxes are shown on the bottom left. Bottom right: Cross-sectional profile of the yellow boxed region and the measured full-width-at-half-maximum (FWHM). (d) Measured width (FWHM) from the localization density distributions and one-dimensional localization density derived from the composite STORM images for ten 1 μm microtubules labeled with Alexa Fluor 647 in the presence of different types of photoswitching reagents. ($n=10$, mean±SD) (e) Resolution measurement of STORM images in the presence of various photoswitching reagents: Fourier ring correlation (FRC) (left) and decorrelation analysis (right). ($n=10$, mean±SD) (f) (Top) Representative STORM images of mitochondria (left) and clathrin-coated pit (CCP, right) labeled with Alexa Fluor 647 in the presence of different types of photoswitching reagents. (Bottom) Cross-sectional profile of mitochondria and radial distribution of CCP from each STORM image, showing the hollowness of each structure. (g) Representative STORM images of microtubules (left), mitochondria (middle), and CCP (right) labeled with Alexa Fluor 647 in the presence of 50 mM NaN_3. Magnified images of red, dashed boxes are shown on the top right. Bottom right: Cross-sectional (for microtubule and mitochondria) or radial distribution profile (for CCP) of the yellow boxed region and the measured FWHM. White dashed line in CCP image: cell membrane boundary. (h) Resolution measurement of STORM images in the presence of NaN_3 as a photoswitching reagent: FRC (left) and decorrelation analysis (right). ($n=10$, mean±SD) Scale bar: 5 μm in (c) and (g) and 500 nm in (f) and the red boxed region in (c) and (g).

many PSFs overlapped, resulting in incorrect puncta localization in the microtubule filament, as shown in Figure 3c. In addition, the long lifetime of the fluorescence-off state of the dye in the presence of the Type 4 reagent contributes to reducing the number of photoswitching cycles, deteriorating the STORM image quality. The variation in resolution observed in STORM images depending on the type of photoswitching reagent was also confirmed through Fourier

ring correlation (FRC)[29] and decorrelation analyses,[30] both of which are well-established methods for measuring the resolution of super-resolved images. As shown in Figure 3e, we obtained 21 and 25 (Type 1), 25 and 32 (Type 2), 23 and 28 (Type 3), and 65 and 80 nm (Type 4) as resolutions from the FRC and decorrelation analyses, respectively. These results suggest that Type 1 exhibits the best STORM image quality, in contrast to Type 4. We also performed STORM imaging with different types of photoswitching reagents for various biological structures, including mitochondria and CCPs. As shown in Figure 3f and Figure S5, the Type 1 reagent revealed a clear hollow structure of mitochondria and CCPs owing to its faster photoswitching rates with short τ_{on} and τ_{off}, whereas this hollow structure was not significantly visualized, particularly when the Type 4 reagent was used, owing to its longest τ_{on} and τ_{off} among the reagent types. This implies that Type 1 has good photoswitching properties and Type 4 has the worst photoswitching properties for super-resolution imaging in general. Therefore, we observed the effect of the photoswitching reagents on the STORM image quality of biological samples in a manner consistent with our single-molecule measurements.

Finally, the optimal photoswitching reagent was determined based on the systematic investigation of the effect on the STORM image quality. Although thiols have been widely used as photoswitching reagents, it is important to find other suitable photoswitching reagents for cases where alternatives to thiols are needed. Therefore, we attempted to identify another photoswitching reagent based on the systematic investigation of various photoswitching reagents. The results indicate that a photoswitching reagent with weak binding energy to the dye molecule and good nucleophilicity can induce fast photoswitching of the dye, resulting in high-resolution STORM images. In this regard, NaN_3 was expected to be a good photoswitching reagent because the azide ion (N_3^-) has good nucleophilicity and binds weakly to the dye molecule (191 kJ/mol). By varying the imaging buffer conditions, including the pH and concentration, the photoswitching of the dye in the presence of NaN_3 was optimized to obtain fast k_{on} and k_{off} for the dye molecule. As shown in Figure 3g, each microtubule filament imaged with NaN_3 was well-resolved, revealing a narrow width and hollow structure. Such a good super-resolution imaging capability of NaN_3 was also successfully demonstrated for STORM imaging of mitochondria and CCPs (Figure 3g). In contrast to Type 2–4, STORM images obtained with NaN_3 revealed the clear hollowness of mitochondria and CCPs, suggesting that NaN_3 can be broadly applied to biological targets. We also conducted FRC and decorrelation analyses for the STORM images of microtubules, mitochondria, and CCPs. As shown in Figure 3h, the resolution of the STORM images obtained with NaN_3 was comparable to that obtained with Type 1, suggesting that NaN_3 serves as an efficient photoswitching reagent. Therefore, we could confirm the super-resolution imaging capability of NaN_3 as a good photoswitching reagent, similar to thiols. In such a way, the present study of the photoswitching mechanism provides guidelines for finding suitable alternative photoswitching reagents to thiols.

Conclusion

In this study, the photoswitching dynamics of fluorophores were investigated in the presence of various photoswitching reagents. The main factors determining each rate were investigated by quantifying the rates of the on-to-off and off-to-on photoswitching processes for AF647 aided by various photoswitching reagents. For example, the nucleophilicity of the photoswitching reagents, which is mainly determined by steric hindrance and substituents, plays an important role in determining the fluorescence on-to-off rate because this process occurs via the nucleophilic addition of a photoswitching reagent to a conjugated bond in the dye molecule. The laser power dependence of the switching-off rate suggests two-photon-induced dissociation of the fluorophore-photoswitching reagent pair, suggesting that the bond dissociation energy of this pair is the main factor determining the fluorescence recovery rate and number of switching cycles. Theoretical calculations indicate that the excited energy level exhibits a dissociative curve, which has not been previously reported. Therefore, the dye-photoswitching reagent pair can be easily dissociated once it is excited to this dissociative energy level by two red photons or one blue photon. Collectively, these results suggest that the fast switching on and off phenomena required to obtain high-quality STORM images can be achieved using a photoswitching reagent with good nucleophilicity and weak binding energy to the dye molecule. However, it should be noted that such an our photoswitching mechanism lies on the assumption that photoswitching reagent is added to the conjugated bond in the polymethine bridge, forming a non-emissive photoproduct. Therefore, our claim may not be applicable to dye molecules that cannot form a photoswitching reagent adduct, such as Cy3 with a shorter polymethine bridge and Cy3B with a rigid structure, as previously reported,[20,21] requiring further investigation of different types of dyes using different approaches.

Based on this systematic investigation of various photoswitching reagents, NaN_3 was tested as a new photoswitching reagent because the azide ion (N_3^-) has good nucleophilicity and a weak binding energy to the dye molecule. As expected, fast photoswitching on and off dynamics were observed when NaN_3 was used as the photoswitching reagent, resulting in well-resolved PSFs of single molecules without overlapping and generating high STORM image quality. We expect that the photoswitching properties can be further improved by optimizing the composition of the imaging buffer, such as the pH and concentration, and the illumination conditions, such as the laser power and wavelength. While previous SMLM studies have considered only thiol as a photoswitching agent, this study not only enables expansion to more classes of photoswitching agents but also improves the SMLM image quality by providing guidelines for the optimal design of new photoswitching agents and imaging conditions.

Acknowledgements

This work was supported by the National Research Foundation of Korea (NRF) Grant funded by the Korea government (MSIT) (no. 2021R1C1C1006700) and Korea Toray Science Foundation (2023).

Conflict of Interest

The authors declare no conflict of interest.

Data Availability Statement

The data that support the findings of this study are available from the corresponding author upon reasonable request.

Keywords: Photoswitching mechanism · Photoswitching reagent · Single-molecule localization microscopy · Super-resolution microscopy

[1] S. W. Hell, J. Wichmann, *Opt. Lett.* **1994**, *19*, 780–782.
[2] M. Hofmann, C. Eggeling, S. Jakobs, S. W. Hell, *Proc. Natl. Acad. Sci. USA* **2005**, *102*, 17565–17569.
[3] M. G. Gustafsson, *Proc. Natl. Acad. Sci. USA* **2005**, *102*, 13081–13086.
[4] M. J. Rust, M. Bates, X. Zhuang, *Nat. Methods* **2006**, *3*, 793–796.
[5] E. Betzig, G. H. Patterson, R. Sougrat, O. W. Lindwasser, S. Olenych, J. S. Bonifacino, M. W. Davidson, J. Lippincott-Schwartz, H. F. Hess, *Science* **2006**, *313*, 1642–1645.
[6] M. Lelek, M. T. Gyparaki, G. Beliu, F. Schueder, J. Griffié, S. Manley, R. Jungmann, M. Sauer, M. Lakadamyali, C. Zimmer, *Nat. Rev. Methods Primers* **2021**, *1*, 39.
[7] S. T. Hess, T. P. Girirajan, M. D. Mason, *Biophys. J.* **2006**, *91*, 4258–4272.
[8] J. Lippincott-Schwartz, S. Manley, *Nat. Methods* **2009**, *6*, 21–23.
[9] D. Jeong, D. Kim, *Mol. Cells* **2022**, *45*, 41.
[10] M. N. Bongiovanni, J. Godet, M. H. Horrocks, L. Tosatto, A. R. Carr, D. C. Wirthensohn, R. T. Ranasinghe, J.-E. Lee, A. Ponjavic, J. V. Fritz, *Nat. Commun.* **2016**, *7*, 13544.
[11] D. Wöll, C. Flors, *Small Methods* **2017**, *1*, 1700191.
[12] D. T. Nguyen, S. Mun, H. Park, U. Jeong, G.-h. Kim, S. Lee, C.-S. Jun, M. M. Sung, D. Kim, *Nano Lett.* **2022**, *22*, 10080–10087.
[13] Y. Park, D. Jeong, U. Jeong, H. Park, S. Yoon, M. Kang, D. Kim, *ACS Appl. Mater. Interfaces* **2022**, *14*, 46032–46042.
[14] U. Jeong, D. Jeong, S. Go, H. Park, G.-h. Kim, N. Kim, J. Jung, W. Kim, M. Lee, C. Choi, *Chem. Mater.* **2023**, *35*, 5572–5581.
[15] X. Zhuang, *Nat. Photonics* **2009**, *3*, 365–367.
[16] J. C. Vaughan, S. Jia, X. Zhuang, *Nat. Methods* **2012**, *9*, 1181–1184.
[17] H. Li, J. C. Vaughan, *Chem. Rev.* **2018**, *118*, 9412–9454.
[18] A. Shivanandan, H. Deschout, M. Scarselli, A. Radenovic, *FEBS Lett.* **2014**, *588*, 3595–3602.
[19] G. T. Dempsey, J. C. Vaughan, K. H. Chen, M. Bates, X. Zhuang, *Nat. Methods* **2011**, *8*, 1027–1036.
[20] G. T. Dempsey, M. Bates, W. E. Kowtoniuk, D. R. Liu, R. Y. Tsien, X. Zhuang, *J. Am. Chem. Soc.* **2009**, *131*, 18192–18193.
[21] Y. Gidi, L. Payne, V. Glembockyte, M. S. Michie, M. J. Schnermann, G. Cosa, *J. Am. Chem. Soc.* **2020**, *142*, 12681–12689.
[22] I. H. Stein, S. Capone, J. H. Smit, F. Baumann, T. Cordes, P. Tinnefeld, *ChemPhysChem* **2012**, *13*, 931–937.
[23] K. Klehs, C. Spahn, U. Endesfelder, S. F. Lee, A. Fürstenberg, M. Heilemann, *ChemPhysChem* **2014**, *15*, 637–641.
[24] L. Herdly, P. W. Tinning, A. Geiser, H. Taylor, G. W. Gould, S. van de Linde, *J. Phys. Chem. B* **2023**, *127*, 732–741.
[25] M. Bates, B. Huang, G. T. Dempsey, X. Zhuang, *Science* **2007**, *317*, 1749–1753.
[26] J. Chung, U. Jeong, D. Jeong, S. Go, D. Kim, *Anal. Chem.* **2021**, *94*, 618–627.
[27] A. P. Gorka, R. R. Nani, M. J. Schnermann, *Org. Biomol. Chem.* **2015**, *13*, 7584–7598.
[28] A. Schulz, *Z. Anorg. Allg. Chem.* **2014**, *640*, 2183–2192.
[29] R. P. Nieuwenhuizen, K. A. Lidke, M. Bates, D. L. Puig, D. Grünwald, S. Stallinga, B. Rieger, *Nat. Methods.* **2013**, *10*, 557–562.
[30] A. Descloux, K. S. Grußmayer, A. Radenovic, *Nat. Methods.* **2019**, *16*, 918–924.

Manuscript received: March 17, 2024
Accepted manuscript online: April 15, 2024
Version of record online: May 15, 2024